REAL PHANTOM DATASETS FOR THE EVALUATION OF COMPRESSIVE SENSING BASED INTERIOR SPECT

Baodong Liu[1,2], Akiva Mintz[2], and Hengyong Yu[2,]*

1. Key Lab of Nuclear Analysis Techniques, Institute of High Energy Physics, CAS; and Beijing Engineering Research Center of Radiographic Techniques and Equipment, Beijing 100049, PRC
2. Dept. of Biomedical Engineering, VT-WFU School of Biomedical Engineering and Sciences; and Department of Radiology, Wake Forest University Health Sciences, Winston-Salem, NC 27157, USA
* Corresponding author (Email: hengyong-yu@ieee.org)

ABSTRACT

To significantly improve the temporal resolution for dynamic cardiac imaging, multiple cameras have been proposed to be integrated in a single-photon emission computed tomography (SPECT) system focusing on a heart-size region-of interest (ROI). However, the truncated projections will cause interior SPECT problem, which doesn't have unique solution. Inspired by the recent results on interior tomography in the x-ray computed tomography (CT) field, the compressive sensing (CS)-based interior SPECT theories have been established. However, those theoretical results have not been evaluated using a realistic dataset acquired from a clinical SPECT scanner. In this data paper, we present a phantom dataset acquired from a clinical SPECT scanner and use it to evaluate the CS-based iterative reconstruction algorithm for interior SPECT.

Index Terms—Data Paper, Interior SPECT, Compressive Sensing, Total Variation Minimization, OS-SART

1. INTRODUCTION

In a single-photon emission computed tomography (SPECT) examination, some gamma-emitting radionuclide is first injected into the bloodstream of a patient. Then, a planar gamma camera is rotated around the patient to acquire multiple 2D projections. The 3D distribution of a radionuclide source can be reconstructed from the 2D projections[1, 2]. One of the major drawbacks of the SPECT is its extended imaging time for dynamic imaging. Now, commercial two or three heads SPECT systems have been widely used in clinical. To further reduce the acquisition time and improve the temporal resolution of SPECT, a natural solution is to increase the gamma camera number to acquire multiple projections simultaneously. Consequently, in recent years several dedicated SPECT systems have been developed for dynamic cardiac imaging [3], which has small multiple gamma cameras focusing on a heart-size region-of-interest (ROI).

The computed tomography (CT) reconstruction is a special case of SPECT when the attenuation coefficients are set to zero. Inspired by the recent results on interior tomography in the x-ray CT field, we proved that theoretically exact interior SPECT is feasible from uniformly attenuated local projection data, aided by a known sub-region in an ROI [1]. Based on the compressive sensing (CS) theory, it was proved that if an ROI is piecewise polynomial, then it can be uniquely reconstructed from truncated SPECT data that go directly through the ROI [2]. However, on one hand, those theoretical results have not been evaluated using a realistic dataset acquired from a clinical SPECT scanner. On the other hand, there is no standard real SPECT datasets available. This motivates us to present a standard phantom dataset to serve as a platform for the evaluation of SPECT reconstruction algorithms.

In this data paper, we present a phantom dataset acquired from a clinical SPECT scanner and use it to evaluate the CS-based iterative reconstruction algorithm for interior SPECT. The organization of the paper is the following. In the next section, we define the interior SPECT problem and present an iterative reconstruction method. In section III, we describe the datasets. In section IV, we evaluate the performance of the interior SPECT algorithm using the real phantom datasets. In the last section, we discuss relevant issues and conclude this data paper.

2. INTERIOR SPECT METHOD

2.1. Interior SPECT

Let $f(\mathbf{x})$ be a 2D smooth distribution function on a compact support Ω with $\mathbf{x}=(x_1,x_2)\in\Omega$. In a parallel-beam geometry, a SPECT projection of $f(\mathbf{x})$ in rotation angle θ is [4]

$$P(\theta,s)=\int_{-\infty}^{\infty} f(s\boldsymbol{\theta}+t\boldsymbol{\theta}^{\perp})e^{-\int_t^{\infty}\mu(s\boldsymbol{\theta}+\tilde{t}\boldsymbol{\theta}^{\perp})d\tilde{t}}dt, \quad (1)$$

where $\boldsymbol{\theta}=(\cos\theta,\sin\theta)$, $\boldsymbol{\theta}^{\perp}=(-\sin\theta,\cos\theta)$ and $\mu(\mathbf{x})$ denotes the attenuation map on the whole support. In real

applications, the attenuation map μ is acquired from CT scanner.

The interior SPECT projection of $f(\mathbf{x})$ can be described by [2]

$$P_I(\theta,s)=P(\theta,s),-c<s<c,0\le\theta<2\pi. \quad (2)$$

Figure 1 illustrates the interior SPECT/CT. We can find that in any rotation angle θ, only the central part of the projection are available. According to the results in [2], if $f(\mathbf{x})$ is a piecewise smooth function and compactly supported on a disk $\Omega_r=\{\mathbf{x}=(x_1,x_2)\in\mathbb{R}^2:|\mathbf{x}|<r\}$, and the attenuation map $\mu(\mathbf{x})$ is a constant in Ω_r, then the interior problem (2) has a unique solution $f(\mathbf{x})$ in the ROI region $\Omega_c=\{\mathbf{x}=(x_1,x_2)\in\mathbb{R}^2:|\mathbf{x}|<c<r\}$.

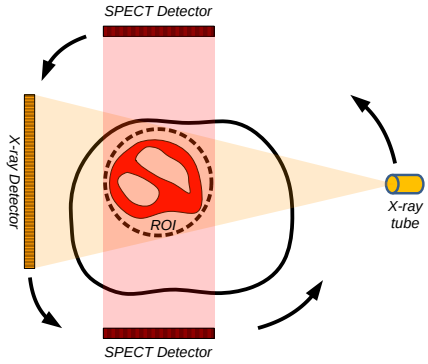

Figure 1. Illustration of the interior SPECT/CT.

2.2. Discrete model of SPECT system

For CT scanning systems, the discrete model of projections in terms of the Radon transform can be expressed as [5]

$$W\mu=b, \quad (3)$$

where $b=(b_1,b_2,...,b_{M_0})^T\in\mathbb{R}^{M_0}$ represents the measured projections and each b_m is measured along an x-ray path, one dimensional (1D) vector $\mu=(\mu_1,\mu_2,...,\mu_{N_0})^T\in\mathbb{R}^{N_0}$ reformatted from the 2D CT image $\mu_{i,j}$ and a known non-zero matrix W whose component $w_{m,n}$ is the intersection area between the *m*th x-ray path and *n*th pixel.

For SPECT scanning system, the discrete model of projections can be expressed as

$$Af=p, \quad (4)$$

where $p=(p_1,p_2,...,p_M)^T\in\mathbb{R}^M$ represents the measured SPECT projections and 1D vector $f=(f_1,f_2,...,f_N)^T\in\mathbb{R}^N$ reformatted from the 2D SPECT image $f_{i,j}$. Suppose the CT image and SPECT image have the same size and let $L_{m,n}$ represent the radial in the *m*th ray and starts from the *n*th pixel, the component $a_{m,n}$ of the matrix A can be expressed as

$$a_{m,n}=w_{m,n}e^{-\sum_{L_{m,n}}w_{m,k}\mu_k}. \quad (5)$$

For interior SPECT system, only the available ray paths are considered.

2.3. CS based iterative reconstruction method

The expectation maximization (EM) algorithm is an iterative procedure to calculate maximum likelihood estimates [6]. The ML-EM algorithm is given by

$$f_n^{(k+1)}=\frac{f_n^{(k)}}{\sum_{m=1}^{M}a_{m,n}}\sum_{m=1}^{M}\frac{a_{m,n}p_m}{\sum_{l=1}^{N}a_{m,l}f_l^{(k)}}, \quad (6)$$

where k represents the iteration number. We can find that each image estimate is updated after all correction term have been backprojected.

Suppose that $f(\mathbf{x})$ is piecewise constant in the ROI Ω_c, it can be reconstructed by minimizing the total variation (TV) of a candidate image [2]. Let $f_{i,j}$ be a digital image reconstructed from the available local projections, where Δ represents the sampling interval, and i and j are integers. Similar to the reconstruction method used in [7], we develop the following reconstruction method:

Initialize iteration number $k=0$ *and* $\mathbf{f}^{(k)}=0$;

Repeat the main loop:

$k=k+1$, $\mathbf{f}^{(k)}=\mathbf{f}^{(k-1)}$;

Update $\mathbf{f}^{(k)}$ *by formula (6);*

Initialize the maximal step for the steepest descent $\rho=0.005$ *and the decreasing scale of* ρ *after each computation* $\rho_s=0.997$;

Repeat TV minimization loop:

Computing the steepest decent direction $d_{i,j}$:

$$d_{i,j}=\frac{\partial f_{\mathrm{TV}}}{\partial f_{i,j}^{(k)}}=\frac{4f_{i,j}^{(k)}-f_{i+1,j}^{(k)}-f_{i-1,j}^{(k)}-f_{i,j+1}^{(k)}-f_{i,j-1}^{(k)}}{\mu_{i,j}}+\frac{f_{i,j}^{(k)}-f_{i+1,j}^{(k)}}{\mu_{i+1,j}}+\frac{f_{i,j}^{(k)}-f_{i-1,j}^{(k)}}{\mu_{i-1,j}}+\frac{f_{i,j}^{(k)}-f_{i,j+1}^{(k)}}{\mu_{i,j+1}}+\frac{f_{i,j}^{(k)}-f_{i,j-1}^{(k)}}{\mu_{i,j-1}}, \quad (7)$$

where $\mu_{i,j}\cong\sqrt{\frac{\left(\begin{array}{c}(f_{i+1,j}^{(k)}-f_{i,j}^{(k)})^2+(f_{i,j}^{(k)}-f_{i-1,j}^{(k)})^2\\+(f_{i,j+1}^{(k)}-f_{i,j}^{(k)})^2+(f_{i,j}^{(k)}-f_{i,j-1}^{(k)})^2\end{array}\right)}{2\Delta^2}+\varepsilon^2}$, (8)

and ε *is a small positive number;*

$$\beta=\max\left(\left|f_{i,j}^{(k)}\right|\right)\Big/\max\left(\left|d_{i,j}\right|\right), \quad (9)$$

$$f_{i,j}^{(k)}=f_{i,j}^{(k)}-\rho\times\beta\times d_{i,j}, \quad (10)$$

$$\rho=\rho\times\rho_s; \quad (11)$$

Until the stopping criteria are satisfied.

In each iteration step, first the ML-EM algorithm is used to enforce data consistency, then the steepest descent search algorithm is used to minimize the TV of the reconstructed image.

3. DATASET DESCRIPTION

3.1. Data acquisition

A Jaszczak SPECT phantom filled with radionuclide was scanned by a Philips BrightView SPECT XCT. 128 projections were uniformly acquired over 360 degree in a parallel-beam geometry. Each projection was in a matrix of 256×256, and the detector element size was 1.598×1.598 mm^2. The projection of the origin was exactly the geometrical center of the detector. A 3D volume CT image was reconstructed by the scanner. It has 256 slices and each slice has 324×324 pixels. The slice thickness and pixel width and height were all 1.598 mm. The origin was also exactly located in the geometrical center of the 3D CT image. Therefore, one CT slice image exactly corresponds to one SPECT slice image and there is no mismatch problem.

3.2. Data format

All data were saved as MATLAB *mat* files. The scanning angles were stored as a 128×1 vector "*Angles"* and saved as "*Angles.mat"*. The 3D CT image data were stored as a 3D 324×324×256 array "*CTImage"* and saved as "*3DCTImage.mat"*. Each page (the 3rd dimension) of *"CTImage"* represents a slice of 2D 324×324 CT image. The projection data were stored as a 3D 256×256×128 array "*SPECTProj"* and saved as "*3DSPECTProj.mat"*. Each page of *"SPECTProj"* represents a 2D 256×256 SPECT projection in a scanning view.

3.3. Method to read

All data can be loaded using MATLAB *load* command.

3.4. Evaluation criteria

For the interior SPECT, the reconstruction results can be quantitatively evaluated using two indices. One is the root mean square error (RMSE), the other is the image quality assessment index for structural similarity (SSIM) [8], which is shown to be consistent with visual perception. The closer it is to 1, the higher the structural similarity is. The images reconstructed from non-truncated global projections can serve as references.

4. EXPERIMENTAL RESULTS

Because the SPECT projections are very noisy, a Butterworth filtering was used to reduce the noises in the projections. In the experiments, 10 slices (#155-164) which cut cold rods were selected.

In the first study, the projections at the 160th row were extracted to form the sinogram for the 160th slice. Figure 2 shows the sinogram without/with Butterworth filtering. The corresponding x-ray CT image was used to serve as an accurate attenuation map for the SPECT reconstruction. Furthermore, the support of the CT image was selected as the support of the SPECT image. At the end of each iteration, the pixels outside the support were set to be zero.

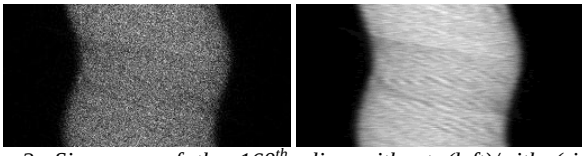

Fig. 2. Sinogram of the 160th slice without (left)/with (right) Butterworth filtering.

In order to simulate an interior problem, we manually truncated the projections to only keep the central 88 detector cells. Figure 3 shows the reconstructed images of the 160th slice. For global reconstruction, the maximum iteration number was 20, while for interior reconstruction it was 100. Figure 4 shows image profiles along the vertical and horizontal central lines. From figures 3 and 4, we can see that the interior SPECT results are in a good match with the global ones. Besides, the CS-based reconstructed results are smoother than the results using EM algorithm.

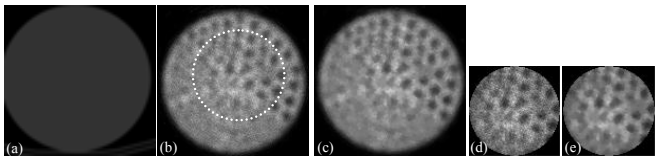

Fig. 3. The reconstructed results of the 160th slice. (a) is the x-ray CT image in a display window [0, 0.1]. (b) and (c) are the SPECT images reconstructed by the EM and CS-based algorithms from global projections, respectively. The white circle in (b) indicates the interior ROI. (d) and (e) are the corresponding interior SPECT images of (b) and (c). The display window for (b)-(e) is [0, 0.7].

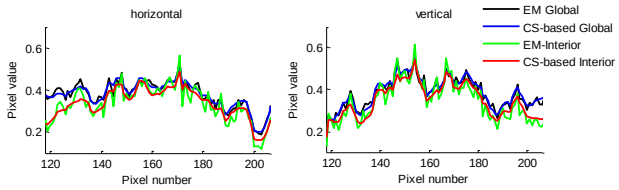

Fig. 4. Profiles along the vertical and horizontal central lines.

In the second study, the other 9 slices were reconstructed and the results were quantitatively evaluated using RMSE and SSIM. The EM global results were considered as benchmarks for the reconstructed images from truncated projections. The RMSE and SSIM indices of these results are plotted in figure 5. From the quantitative comparison, we can find that CS-based algorithm outperforms EM.

In order to observe the iteration process, for each slice from 155 to 164, the RMSEs of the reconstructed images after different numbers of iterations are plotted in figure 6.

We can find that CS-based method has higher precision and faster convergence speed. Furthermore, EM has obvious semiconvergence phenomenon. After about 40 iterations, the RMSEs of EM results become larger, while the RMSEs of CS-based results still become smaller.

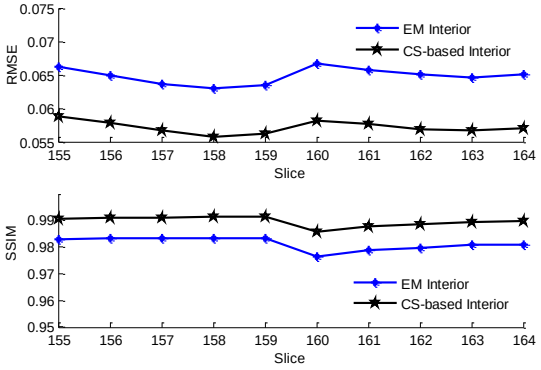

Fig. 5. RMSEs and SSIMs of reconstructed slices from truncated projections.

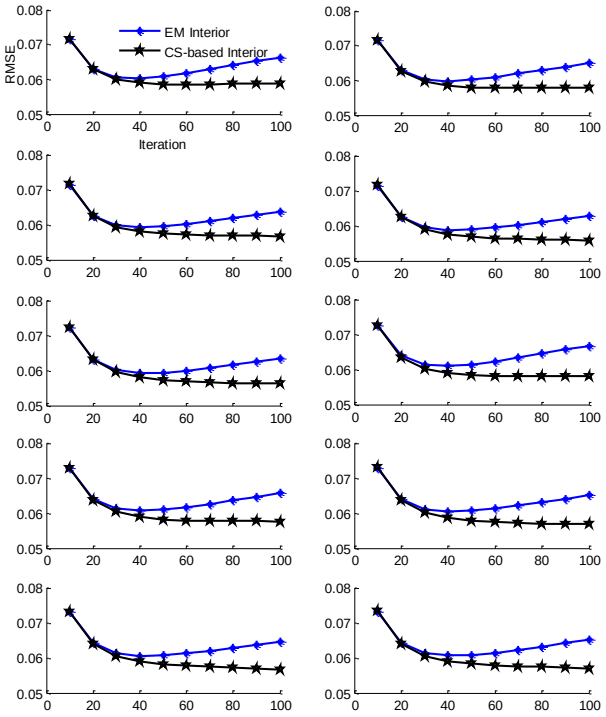

Fig. 6. RMSEs of reconstructed images after different numbers of iterations. From top to bottom and left to right, the plots are corresponding to the 155th to 164th slices.

5. CONCLUSION

The CS-based interior SPECT reconstruction algorithm has been successfully developed and evaluated on phantom experiment. Compared with EM method, the improvement of image quality has been demonstrated. Furthermore, the CS-based method has faster and better convergence.

6. ACKNOWLEGEMENT

This work was partially supported by the NSF/DMS grant 1210967. The work of BD Liu was partially supported by IHEP-CAS Scientific Research Foundation 2013IHEPYJRC801.

7. REFERENCES

[1] H. Yu, J. Yang, M. Jiang, and G. Wang, "Interior SPECT—exact and stable ROI reconstruction from uniformly attenuated local projections," *Communications in numerical methods in engineering*, vol. 25, pp. 693-710, 2009.

[2] J. Yang, H. Yu, M. Jiang, and G. Wang, "High-order total variation minimization for interior SPECT," *Inverse problems*, vol. 28, p. 015001, 2012.

[3] G. T. Gullberg, B. WReutter, A. Sitek, J. S. Maltz, and T. F. Budinger, "Dynamic single photon emission computed tomography—basic principles and cardiac applications," *Phys Med Biol*, vol. 55, pp. R111-191, 2010.

[4] H. Rullgard, "An explicit inversion formula for the exponential Radon transform using data from 180 ~," *Ark. Mat.,*, vol. 42, pp. 353-362, 2004.

[5] G. Wang and M. Jiang, "Ordered-subset simultaneous algebraic reconstruction techniques (OS-SART)," *Journal of X-Ray Science and Technology*, vol. 12, pp. 169-177, 2004.

[6] A. P. Dempster, N. M. Laird, and D. B. Rubin, "Maximum Likelihood from Incomplete Data Via Em Algorithm," *Journal of the Royal Statistical Society Series B-Methodological*, vol. 39, pp. 1-38, 1977.

[7] H. Yu and G. Wang, "Compressed sensing based interior tomography," *Physics in Medicine and Biology*, vol. 54, pp. 2791-2805, May 7 2009.

[8] Z. Wang, A. C. Bovik, H. R. Sheikh, and E. P. Simoncelli, "Image quality assessment: From error visibility to structural similarity," *IEEE Transactions on Image Processing*, vol. 13, pp. 600-612, Apr 2004.

Raw Dataset Available at:
https://drive.google.com/folderview?id=0BzFauoP3UVDFWVMwY0pwenpRY0E&usp=sharing
https://skydrive.live.com/?cid=fd350a2698cab1ec&id=FD350A2698CAB1EC!3106&authkey=!AP4qf1k8NTPJvBE